Mesoporous Materials

DOI: 10.1002/ange.200502332

Crystal-to-Crystal Phase Transition in Self-Assembled Mesoporous Iron Oxide Films**

*Torsten Brezesinski, Matthijs Groenewolt, Markus Antonietti, and Bernd Smarsly**

In the past years, various types of mesoporous metal oxide films featuring crystalline pore walls have been synthesized by our group,[1] but the preparation of mesoporous crystalline iron oxides has remained a challenge. Magnetic nanoparticles of the iron oxides magnetite (Fe_3O_4) and maghemite (γ-Fe_2O_3) are already used for magnetic data storage[2] and biomedical applications,[3] and similar applications are envisaged for magnetic mesoporous materials. Furthermore, mesoporous iron oxide films offer potential as materials for electrodes,[4] (magneto)optical devices,[5] and catalysts.[6] In particular, interest in hematite (α-Fe_2O_3) has increased, owing to its ferrimagnetic behavior, and catalytic and sensoric activity.[7] For all of these applications, homogeneous mesoporous thin films are desirable.

Although nanocrystalline iron oxide aerogels,[8] as well as mesostructured amorphous iron oxides have been synthesized,[9] mesoporous crystalline films have not been reported to date, for several reasons. Firstly, similar to alumina precursors, iron species feature a complex sol–gel behavior and a strong gelation tendency. Secondly, iron oxides display an intricate crystallization behavior, forming a variety of crystalline phases, including many with nonstoichiometric compositions.[10] Thirdly, the preparation of regular mesopore structures by sol–gel processing is further impeded by the fact that these procedures usually lead to the initial formation of goethite (α-FeOOH). This iron oxide modification has to be transformed into another modification through a crystal-to-crystal phase transition, which can potentially disrupt the mesostructure.

Herein, we report the synthesis of crack-free mesoporous α-Fe_2O_3 and α-FeOOH thin films using the evaporation-induced self-assembly (EISA) process and a subsequent, straightforward heat-treatment step. The problems listed above were overcome through the use of appropriate novel block copolymer templates, namely, poly(isobutylene)-*block*-poly(ethylene oxide) (PIB–PEO),[11] which features an ultrahydrophobic poly(isobutylene) block, and the recently developed poly(ethylene-co-butylene)-*b*-poly(ethylene oxide) (KLE).[12] Both block copolymers tolerate the extreme processing conditions in the EISA process. Additionally, the size of the micelles generated by these block copolymers was selected to be larger than those of the pluronic surfactants that are usually applied. Hence, the micelle/pore size was of a suitable dimension to be mapped by nanocrystals without destruction of the mesostructure at the onset of crystallization. A similar process was successfully applied in the preparation of mesoporous nanocrystalline perovskites.[13] However, in contrast to these oxides, iron oxide undergoes a crystal-to-crystal phase transition from goethite to hematite. We, therefore, investigated the mesostructural changes that occur with the phase transition, and the peculiarities of crystallization behavior within mesoscopic confinement.[14]

Transmission electron microscopy (TEM) images obtained after heat treatment of films at 450 °C depict the well-ordered mesostructure, which is composed of pores with an average diameter of approximately 10 nm (Figure 1 a). Moreover, they reveal that the samples are highly homogeneous. The corresponding selected-area electron diffraction (SAED) pattern displays rings characteristic of a structure composed of small domains with their crystallographic axes randomly oriented with respect to one another (Figure 1 b).

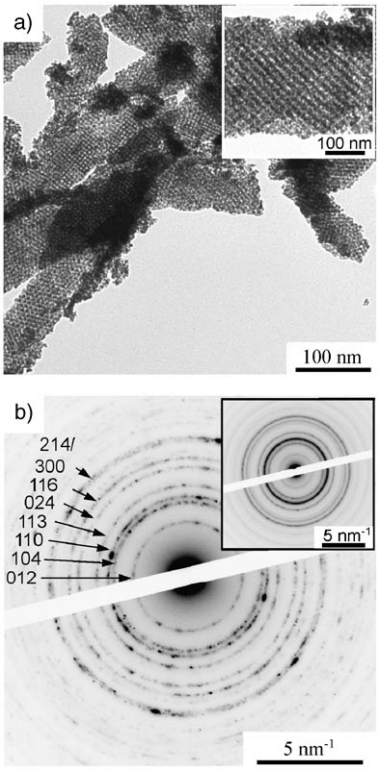

Figure 1. a) TEM images of a mesoporous α-Fe_2O_3 film after heat treatment at 450 °C; the inset is a magnification. b) SAED pattern of the same zone, showing diffraction rings corresponding to the α-phase of Fe_2O_3; the inset depicts the first crystalline modification (α-FeOOH) found at 300 °C.

[*] Dr. T. Brezesinski, Dr. M. Groenewolt, Prof. Dr. M. Antonietti, Dr. B. Smarsly
Max Planck Institute of Colloids and Interfaces
Research Campus Golm
14424 Potsdam (Germany)
Fax: (+49) 331-567-9502
E-mail: bernd.smarsly@mpikg.mpg.de

[**] We thank Prof. Dr. Ken-ichi Iimura for the XPS analyses, Ines Below and Dr. Helmut Schlaad for providing the block copolymers, and Dr. Heinz Amenitsch for help with the in situ 2D-SAXS measurements at the Elettra synchrotron facility in Trieste. Financial support by the Max Planck Society is gratefully acknowledged.

Supporting information for this article is available on the WWW under http://www.angewandte.org or from the author.

 © 2006 Wiley-VCH Verlag GmbH & Co. KGaA, Weinheim

The *d*-spacings could be unambiguously assigned to hematite, the α-phase of Fe_2O_3, which is the most thermodynamically stable form of FeO_x. The crystallite size was determined to be approximately 7–10 nm. At temperatures below 350 °C, SAED revealed that α-FeOOH is formed as the low-temperature modification (Figure 1 b, inset).

Atomic force microscopy (AFM) demonstrated that the pores are accessible from the top and showed the smooth, crack-free surface of the films (see Supporting Information). In addition, Brunnauer–Emmet–Teller (BET) analysis using Krypton as adsorbent (77 K) gave a surface area of 150 $m^2 g^{-1}$, indicating that the majority of the mesopores are accessible.

FeO_x species containing exclusively Fe^{3+} ions were obtained after heat treatment of the films, probably because $FeCl_3$ was employed as the precursor. Various experiments were, therefore, performed in an attempt to generate other species. These experiments involved iron oxide precursors of different valences and thermal treatment of the films under an inert atmosphere. In general, Fe_3O_4, the spinel-type iron oxide, was difficult to obtain by sol–gel processing, as Fe^{2+} tends to oxidize to Fe^{3+}; Fe_3O_4 oxidizes to γ-Fe_2O_3 with preservation of the lattice structure. Because of the poor sol–gel chemistry of Fe^{2+} salts, films of fair optical quality without structuring on the mesoscale were obtained. Interestingly, the use of stoichiometric amounts of Fe^{2+} and Fe^{3+} precursors also resulted in α-Fe_2O_3, demonstrating the distinct sensitivity of Fe^{2+} ions towards oxidation. These findings indicate that the preparation of mesoporous Fe_3O_4 and γ-Fe_2O_3 films by the sol–gel route is substantially more difficult than the synthesis of α-FeOOH and α-Fe_2O_3 films.

To elucidate the influence of mesoscopic confinement on the crystallization behavior, a nonporous powder was prepared without polymer template. Wide-angle X-ray scattering (WAXS) of this reference material revealed that the first crystalline phase formed (goethite) transforms completely into hematite at 300 °C (see Supporting Information).[15] Interestingly, in mesostructured films, this crystal-to-crystal phase transition does not take place below 350 °C, pointing to the retardation of nucleation and crystal growth within the thin walls of the scaffold. The retention of mesostructural order can be attributed to the relatively high thermal stability of the novel block copolymers. Pluronic surfactants, on the other hand, decompose entirely at 350 °C. The PIB–PEO and the KLE porogens were shown to facilitate the preservation of mesoscopic order up to 400–450 °C, that is, during the conversion of the amorphous matrix into its crystalline counterpart.[16]

For direct comparison, thin films were prepared using pluronic F127 to shed more light on the influence of the template stability on mesostructural integrity during the crystal-to-crystal phase transition from α-FeOOH to α-Fe_2O_3. Small-angle X-ray scattering (SAXS) and TEM showed that the use of 30 wt. % porogen, with respect to the amount of α-Fe_2O_3 formed, resulted in films with good optical quality and well-ordered mesostructure (see Supporting Information). Mesostructural collapse was observed at approximately 350 °C, because the complete thermal decomposition of the pluronic template was faster than the recrystallization of the iron oxide matrix. This finding suggests that porogens with higher thermal stability are necessary for the preservation of mesostructure, in the presence of stresses induced by the phase transition.

X-ray photoelectron spectroscopy (XPS) was used to gain further insight into the chemical composition of the mesoporous iron oxide thin films after the onset of crystallization. The XPS data were in good agreement with a reference of almost pure α-Fe_2O_3.[17] Figure 2 demonstrates that the thin

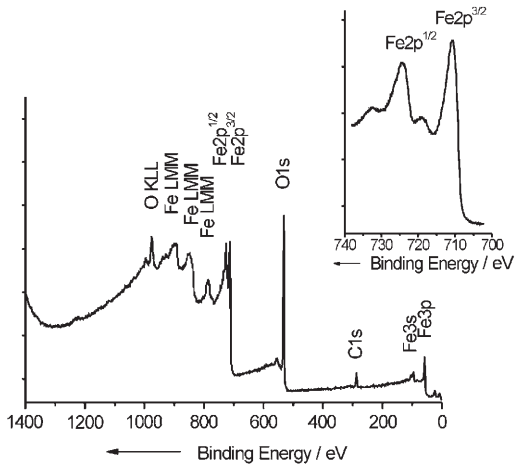

Figure 2. XPS survey spectrum of a mesoporous iron oxide film after heat treatment at 450 °C, confirming the generation of α-Fe_2O_3. The inset is a high-resolution expansion of the Fe2p energy region, showing the complex line shape and the characteristic Fe^{3+} satellite peak.

layers consist of iron, oxygen, and a small amount of contaminating carbon. Moreover, no other impurities, such as chlorides arising from the use of the $FeCl_3$ precursor, could be detected. The $Fe2p^{3/2}$ binding energy of 710.8 eV and the corresponding satellite peak at 718.8 eV, a result of charge transfer screening, can be solely attributed to the presence of Fe^{3+} ions of α-Fe_2O_3. The ratio of atomic concentrations calculated from the O1s and Fe2p peak areas deviates slightly from the theoretical value of 1.5, but it has been reported that quantitative analysis of the XPS data of iron oxides involves certain difficulties (such as, OH groups on the surface and photoreduction of Fe^{3+}).[17]

The temperature-dependent evolution of the mesostructure was also investigated by in situ 2D-SAXS, using a charge-coupled device (CCD) camera (Figure 3), and by 1D-SAXS in symmetric reflection mode, using an energy-dispersive detector (Figure 4). At a temperature of 100 °C, the typical 2D-SAXS scattering pattern of a distorted cubic arrangement of micelles is observed. Similar patterns have been observed for metal oxide systems made with the KLE block copolymer.[1,13] Up to 450 °C, the 2D-SAXS patterns become increasingly ellipsoidal, indicating an anisotropic shrinkage of the mesostructure, in the direction normal to the substrate. Evidently, the transition from α-FeOOH to α-Fe_2O_3 does not affect the mesoscopic order at all, as indicated by the relatively unchanged 2D-SAXS patterns below 450 °C. This finding is remarkable in light of the mechanical stresses that accompany crystal-to-crystal phase transitions. At 600 °C, only broad signals are observed, suggesting degradation of the meso-

 © 2006 Wiley-VCH Verlag GmbH & Co. KGaA, Weinheim

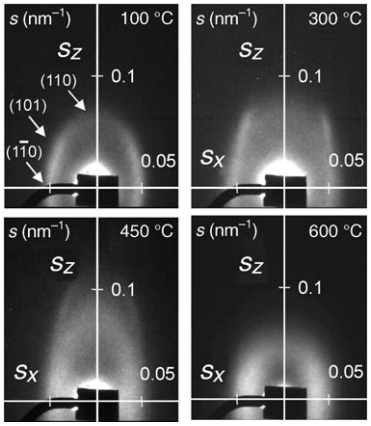

Figure 3. In situ 2D-SAXS measurements, performed during thermal treatment of an iron oxide film, demonstrate the evolution of the bcc arrangement of mesopores as a function of temperature. The scattering patterns are blurred owing to the X-ray fluorescence of iron oxide.

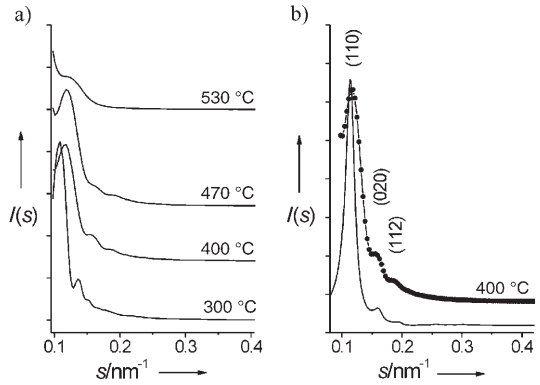

Figure 4. a) 1D-SAXS patterns of mesoporous iron oxide films obtained during various heat-treatment steps. b) Experimental 1D-SAXS pattern of a film treated at 400 °C (circles, line to guide the eye) and the corresponding curve fitting (solid line), which is displaced from the experimental curve for better visualization.

structural order because of diffuse sintering of the nanocrystallites. Thus, the 2D-SAXS patterns demonstrate that an intact cubic mesostructure exists up to temperatures of at least 450 °C.

The 1D-SAXS pattern of a sample heat treated at 400 °C (that is, after the crystal-to-crystal phase transition) displays a sequence of interference maxima, which are attributed to the (110), (020), and (112) reflections of a bcc arrangement of mesopores (Figure 4b). These reflections are in apparent contradiction to the [110] orientation observed in 2D-SAXS, but can be explained by the slit-shaped beam profile of the 1D-SAXS setup used.[18] A recently described procedure was used to quantitatively analyze the lattice parameter and the mesopore size.[12,19] This method provides an average pore diameter of 8 nm and a lattice parameter of 14 nm in the direction normal to the substrate. Note that the reflections are observable up to 470 °C, indicating the regularity of the pore arrangement even at elevated temperatures.

In summary, this study suggests that mesoporous films composed of nanocrystalline phase-pure α-Fe_2O_3 can be obtained by the EISA process using novel block copolymer templates. Porogens featuring a high hydrophilic–hydrophobic contrast and a relatively high thermal stability, such as PIB–PEO and KLE, were able to stabilize the mesostructured scaffold during conversion of the lattice structure from α-FeOOH into α-Fe_2O_3. Hence, the approach described herein could present a general strategy for the preparation of mesoporous films of other metal oxides that undergo crystal-to-crystal phase transitions.

Experimental Section

PIB–PEO (85 mg) was dissolved in EtOH (2 mL) and added to a solution containing $FeCl_3$ (400 mg) and H_2O (300 mg) in a mixture of THF (1 mL) and EtOH (4 mL). The resulting isotropic sol was stirred for 6 h before it was used. Mesostructured thin films were prepared by dip-coating silicon substrates or glass at a constant withdrawal rate (6 mm s^{-1}) and relative humidity (15–20%). Finally, mesoporous crystalline FeO_x films were obtained through controlled nanocrystallization, by heating with a ramp of 5 °C min^{-1} in air. For the in situ 2D-SAXS experiments the heating ramp was adjusted to 10 °C min^{-1} (no significant difference was observed for the different heating rates).

Received: July 4, 2005
Revised: September 29, 2005
Published online: December 21, 2005

Keywords: electron microscopy · iron oxide · mesoporous materials · phase transitions · self-assembly

[1] a) T. Brezesinski, C. Erpen, K. Iimura, B. Smarsly, *Chem. Mater.* **2005**, *17*, 1683–1690; b) M. Kuemmel, D. Grosso, C. Boissière, B. Smarsly, T. Brezesinski, P. A. Albouy, H. Amenitsch, C. Sanchez, *Angew. Chem.* **2005**, *117*, 4665–4668; *Angew. Chem. Int. Ed.* **2005**, *44*, 4589–4592.
[2] Q. A. Pankhurst, R. J. Pollard, *J. Phys. Condens. Matter* **1993**, *5*, 8487–8508.
[3] Q. A. Pankhurst, J. Connolly, S. K. Jones, J. Dobson, *J. Phys. D* **2003**, *36*, R167–R181.
[4] P. Poizot, S. Laruelle, S. Grugeon, L. Dupont, J. M. Tarascon, *Nature* **2000**, *407*, 496.
[5] D. R. Rolison, *Science* **2003**, *299*, 1698.
[6] a) L. Y. Wang, L. Han, J. Luo, C. I. Zhong, *Abstr. Pap. Am. Chem. Soc.* **2004**, *228*, U473–U473; b) B. V. Reddy, S. N. Khanna, *Phys. Rev. Lett.* **2004**, *93*, 068301.
[7] a) D. H. Chen, D. R. Chen, X. L. Jiao, Y. T. Zhao, *J. Mater. Chem.* **2003**, *13*, 2266–2270; b) M. Pelino, C. Colella, C. Canatalini, M. Faccio, G. Ferri, A. Damico, *Sens. Actuators B* **1992**, *7*, 464–469.
[8] J. W. Long, M. S. Logan, C. P. Rhodes, E. E. Carpenter, R. M. Stroud, D. R. Rolison, *J. Am. Chem. Soc.* **2004**, *126*, 16879–16889.
[9] a) F. Jiao, P. G. Bruce, *Angew. Chem.* **2004**, *116*, 6084–6087; *Angew. Chem. Int. Ed.* **2004**, *43*, 5958–5961; b) G. Wirnsberger, K. Gatterer, P. Behrens, *J. Mater. Chem.* **1998**, *8*, 1509–1510.
[10] A. F. Holleman, E. Wiberg, *Lehrbuch der Anorganischen Chemie*, de Gruyter, Berlin, **1995**.
[11] M. Groenewolt, T. Brezesinski, H. Schlaad, M. Antonietti, P. G. Groh, B. Ivan, *Adv. Mater.* **2005**, *17*, 1158–1162.
[12] A. Thomas, H. Schlaad, B. Smarsly, M. Antonietti, *Langmuir* **2003**, *19*, 4455–4459.
[13] D. Grosso, C. Boissière, B. Smarsly, T. Brezesinski, N. Pinna, P. A. Albouy, H. Amenitsch, M. Antonietti, C. Sanchez, *Nat. Mater.* **2004**, *3*, 787–792.

 © 2006 Wiley-VCH Verlag GmbH & Co. KGaA, Weinheim

[14] P. D. Yang, D. Y. Zhao, D. I. Margolese, B. F. Chmelka, G. D. Stucky, *Nature* **1998**, *396*, 152 – 155.
[15] A. F. Gualtieri, P. Venturelli, *Am. Mineral.* **1999**, *84*, 895 – 904.
[16] T. Brezesinski, B. Smarsly, K. Iimura, D. Grosso, C. Boissière, M. Antonietti, C. Sanchez, *Small* **2005**, *1*, 889 – 898.
[17] a) S. Gota, E. Guiot, M. Henriot, M. G. Soyer, *Phys. Rev. B* **1999**, *60*, 14387 – 14395; b) Q. X. Wang, H. B. Pan, B. Z. Song, H. Z. Li, *J. Inorg. Mater.* **2002**, *17*, 782 – 786.
[18] H. Miyata, T. Noma, M. Watanabe, K. Kuroda, *Chem. Mater.* **2002**, *14*, 766 – 772.
[19] B. Smarsly, C. Göltner, M. Antonietti, W. Ruland, E. Hoinkis, *J. Phys. Chem. B* **2001**, *105*, 831 – 840.

 © 2006 Wiley-VCH Verlag GmbH & Co. KGaA, Weinheim